Supporting Information

Guskov et al. 10.1073/pnas.1210076109

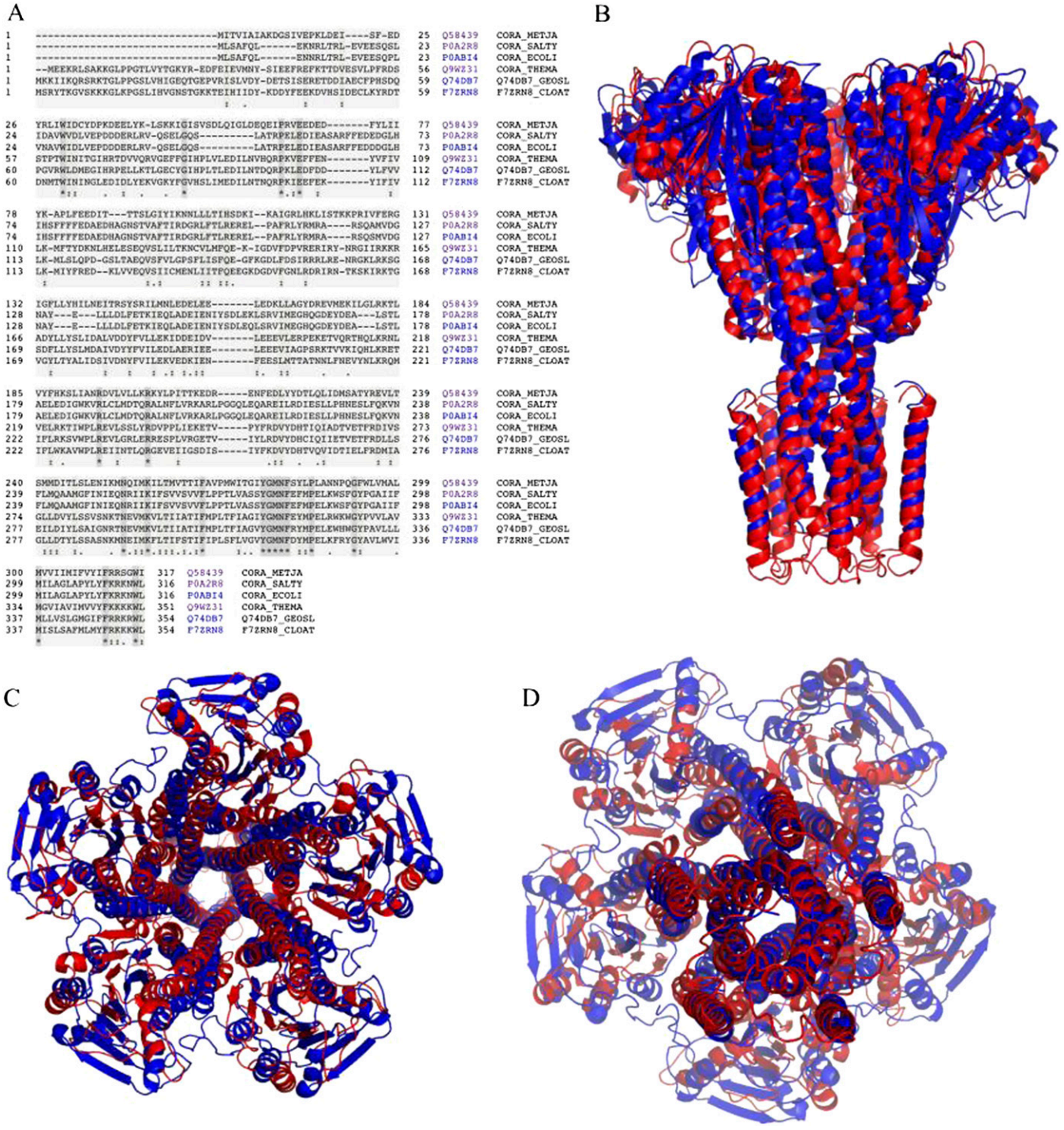

Fig. S1. Structural comparison between Mg^{2+} transporter CorA from the Archaea *Methanocaldococcus jannaschii* and *Thermotoga maritima* (MjCorA and TmCorA, respectively). (*A*) Amino acid sequence alignment of MjCorA and TmCorA along with four other CorA homologs from *Escherichia coli*, *Salmonella typhimurium*, *Geobacter metallireducens*, and *Clostridium acetobutylicum*. (*B*) Side view, (*C*) cytoplasmic view, and (*D*) the extraplasmic view of the superimposition of MjCorA (red) with TmCorA (blue). The rmsd is ~10 Å.

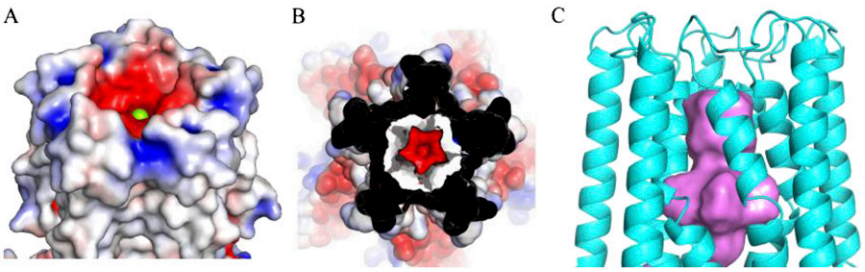

Fig. S2. Internal cavity. (*A*) Extraplasmic view onto the concavity, the same representation as in Fig. 2*D*. (*B*). The cross-section at the T264-ring is shown. (*C*) The internal cavity is highlighted in magenta. Protein subunits are in cyan. Note the helix kink.

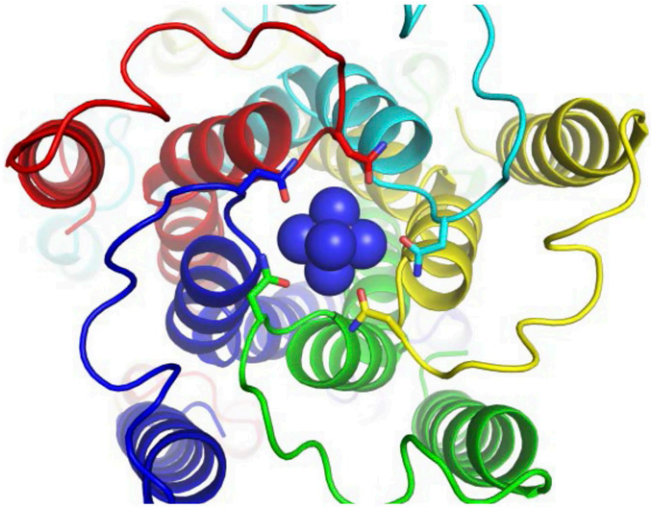

Fig. S3. Possible blockage of the selectivity filter by cobalt(III)hexamine. Cobalt(III)hexamine is well-known inhibitor of transport activity for CorA family. The manual docking of cobalt(III)hexamine and architecture of the selectivity filter suggest it to block the passage and thus prevent any transport.

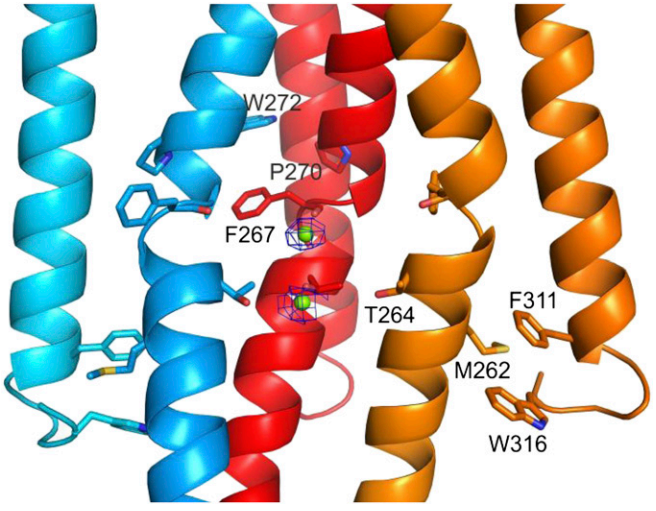

Fig. S4. The T264-ring. Close view onto Thr264 and Phe267 rings. Two Mg^{2+} ions are shown as green spheres with 2 F_o-F_c electron density contoured at 1.5 σ. Two monomers are omitted for clarity. Note that the kink caused by P270 in the helix is enhanced by pulling of Phe267 by Trp272 from an adjacent subunit.

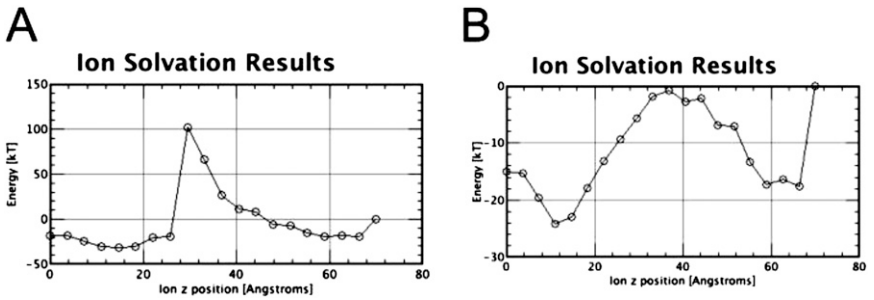

Fig. S5. Ion permeation profile. (*A*) Closed conformation. Note the significant energetic barrier caused by the hydrophobic lock. (*B*) Putative open form with the energetic barrier removed. Both graphs generated by APBSmem.

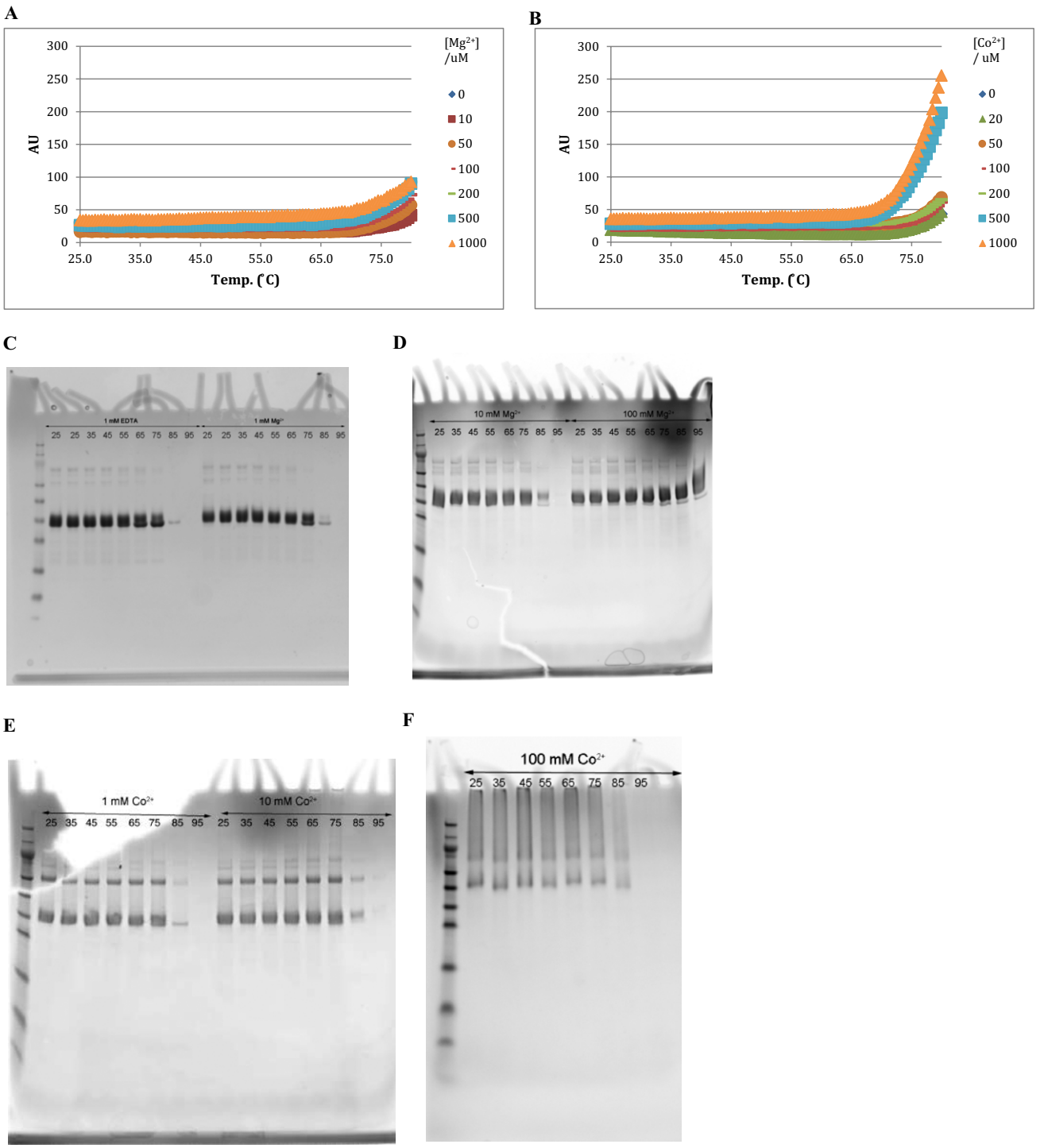

Fig. S6. Thermostability of MjCorA in the presence of Mg^{2+} and Co^{2+}. Thermal shift assay of MjCorA in the presence of up to 1 mM of (*A*) Mg^{2+} and (*B*) Co^{2+} indicates no thermal stabilizing effect of the metal ions. The arbitrary unit (AU) correlates to the level of aggregated protein detected by light scattering, and the scales are adjusted for better comparison. (*C–F*) Coomassie-stained SDS/PAGE analyses of MjCorA recovered after the incubation with EDTA, Mg^{2+} or Co^{2+} at various concentrations and at the indicated temperatures. A slight band shift to higher molecular weight was observed on the SDS/PAGE, which became dominant at 100 mM Mg^{2+}. Co^{2+} showed a destabilizing effect, which is in contrast to its effect on TmCorA (1).

1. Xia Y, et al. (2011) Co2+ selectivity of *Thermotoga maritima* CorA and its inability to regulate Mg2+ homeostasis present a new class of CorA proteins. *J Biol Chem* 286(18):16525–16532.

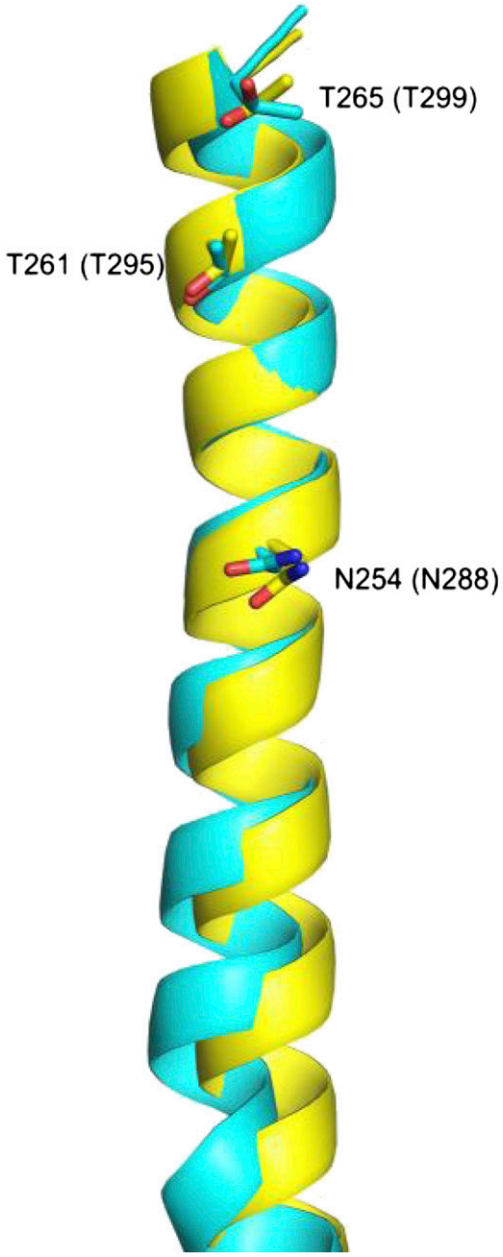

Fig. S7. Superposition of helix-6 (MjCorA, yellow) with helix-7 (TmCorA, cyan). The hydrophilic residues suggested to be involved in ion transport are shown as sticks (numbering in the parentheses is for TmCorA). The rmsd is ~1.2 Å.

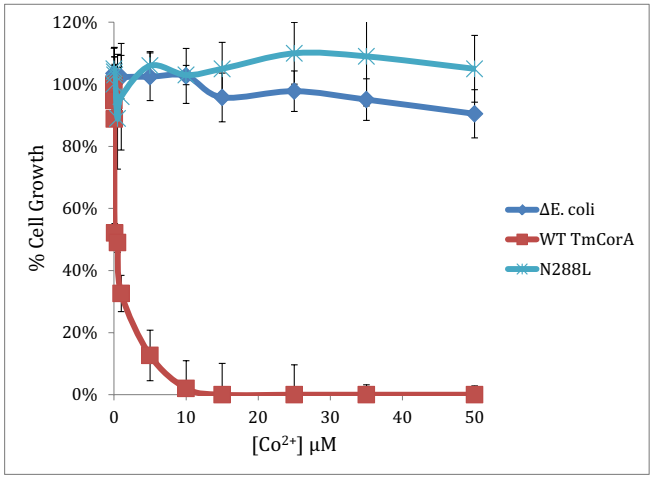

Fig. S8. Assaying the sensitivity of TmCorA toward Co^{2+}. The growth activity of a *corA*-less *E. coli* strain was monitored in the presence of various Co^{2+} concentrations. The *E. coli* strain was transformed with either the wild-type *tmcorA* (WT TmCorA) or the mutated gene for N288L. As the negative control, transformation was done with the empty pBAD vector (Δ*E. coli*). A reduction in the growth activity upon Co^{2+} concentration increase is indicative of the Co^{2+} transport activity of the TmCorA variant. The presented data points are the average of three independent experiments.

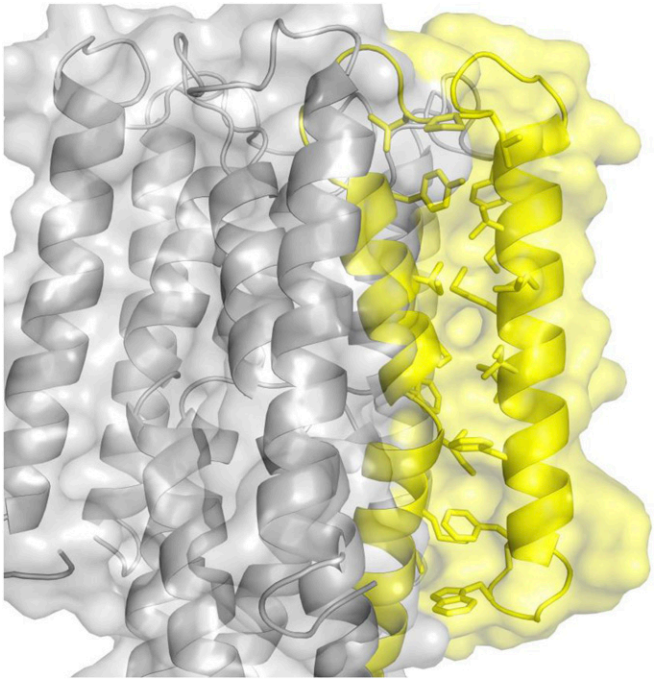

Fig. S9. The tight hydrophobic interaction between transmembrane helices (TM)1 and TM2. TM1 and TM2 of one monomer is colored in yellow; the rest of the protein is in gray. Numerous hydrophobic residues involved in the elongated hydrophobic interface between two TMs are shown as sticks.

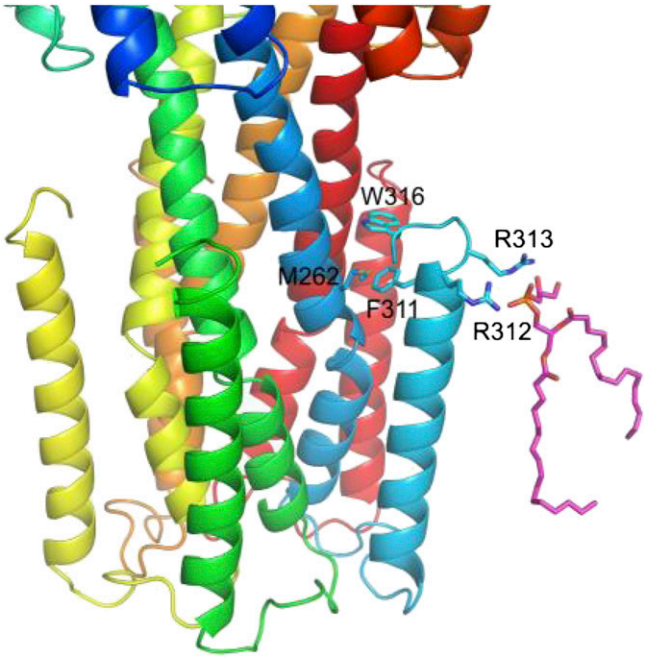

Fig. S10. Possible fixation of TM2 in the lipid matrix. The fixation of TM2 is most possibly facilitated by the salt-bridge formation between R312, R313, and the negatively charged head groups of lipids of the cytoplasmic membrane. The modeled lipid molecule (in stick) is just for illustration of this possibility. F311 and W316 on TM2 interact with and hold M271 on TM1.

Table S1. Data collection and refinement statistics (highest resolution shell is shown in parentheses)

Data and refinement statistics	Native-soluble	SeMet-soluble	Native full-length
Data collection			
Space group	$P6_1$	$P6_122$	$P2_1$
Cell dimensions			
a, b, c (Å)	68.3, 68.3, 241.9	66.8, 66.8, 248.6	103.1, 124.8, 111.9
α, β, γ (°)	90.0, 90.0, 120.0	90.0, 90.0, 120.	90.0, 90.8, 90.0
Numbers of reflections measured	492,488	61,235	198,461
Number of unique reflections	21,977	6,231	46,818
Resolution (Å)	50–2.5 (2.6–2.5)	50–4 (4.1–4)	50–3.2 (3.3–3.2)
R_{merge}	0.1 (0.94)	0.05 (0.36)	0.16 (0.98)
I/σI	31.5 (2.6)	28 (4.7)	7.9 (1.08)
Completeness (%)	99.8 (99.8)	94.1 (99.9)	99.8 (99.8)
Redundancy	22.4 (8.75)	9.2 (4.8)	4.23 (4.2)
Refinement			
Resolution (Å)	47.7–2.5		49.5–3.2
No. reflections (test set)	21,977 (1,099)		46,813 (2,343)
R_{work}/ R_{free}	15.3/19.5		20.9/28.2
No. atoms			
Protein	4,144		12,981
Ligand/ion	193 (alcohols)		223/35 detergent/Mg^{2+}
Water	96		197
B-factors			
Protein	68.1		94.2
Ligand/ion	74.5		158.7/84.2
Water	51.4		61.7
R.m.s deviations			
Bond lengths (Å)	0.007		0.010
Bond angles (°)	1.34		1.50
Ramachandran plot statistics (%)			
Favored regions	95.8		89.9
Allowed regions	4.2		10.1
Disallowed regions	0.0		0.0